Simulation of gravel transport in bypass tunnel during sediment bypass operation of Asahi Dam

Yoji Kubota, Nozomu Yoneyama and Tetsuya Sumi

Abstract

Sediment bypass tunnel is effective sediment countermeasure to reduce sediment inflow into the reservoir and supply sediment downstream of the dam. However, the gravel passing downstream while colliding in the bypass tunnel causes abrasion of the concrete inside the tunnel. Once the operation of the bypass facility is started, the investigation and repair of the abrasion inside the tunnel will be sustained. In order to maintain and manage the bypass tunnel over the long term, establishment of a method for predicting the abrasion area and the amount of wear in the tunnel by gravel is required. In this study, simulation of gravel passing through the tunnel was proposed to predict high frequency of abrasion area in the tunnel. Targeting the bypass tunnel of Asahi Dam in Japan, supercritical flow in the tunnel was analyzed using a three-dimensional flow model and using the calculation result of flow, particle tracking that can reproducing gravel behavior was simulated. Based on both simulation results and observations of tunnel abrasion, the influence of particle size on the migration path of gravel passing through the tunnel was investigated.

Keywords: abrasion, sediment bypassing, three-dimensional model, particle tracking

1   Introduction

Toward the establishment of simulation technology for prediction of abrasion and deterioration due to gravel in the tunnel, based on the simulation results of the three dimensional flow in the tunnel, an analytical model was constructed that performs particle tracking analysis simulating the behavior of gravel. Particle tracking calculation of gravel in the tunnel was conducted for the sediment bypass tunnel of the Asahi Dam in the Shingu River (see Figure 1), and the relationship between the particle size and the migration path of the gravel was investigated from the analysis result.
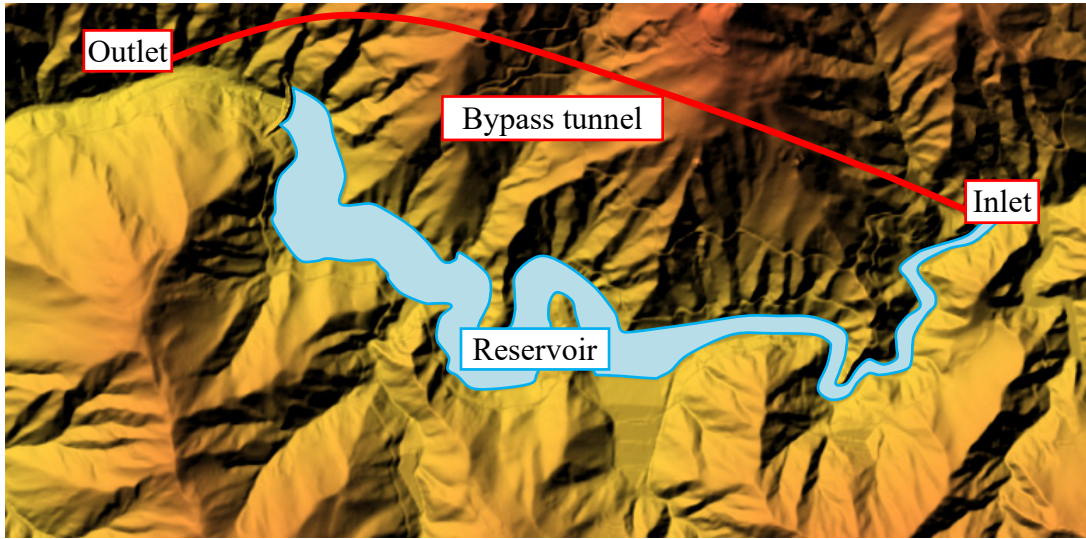
Figure 1: Plan view of the bypass tunnel at the Asahi Dam

2 Numerical modeling of bypass facility flow and sediment transport analysis

2.1 Flow model

In this study, an analytical model incorporating the sediment transport process was used based on the three-dimensional non-hydrostatic pressure analysis model with the Reynolds averaged Navier-Stokes equation as the basic equation developed by Yoneyama *et al.* (2001). According to the verification calculation by Kubota *et al.* (2015), it has been confirmed that this analysis model can reproduce the splitting characteristics of water and sediment to bypass, when sediment transport and diversion flow rate are changed around the diversion weir. Continuous equation [1] and equation of motion [2], which are fundamental equations of flow, are shown below. The basic formula is described by Einstein's summary convention in tensor notation.

$$\frac{\partial u_i}{\partial x_i} = 0 \qquad\qquad [1]$$

$$\frac{\partial u_i}{\partial t} + u\frac{\partial u_i}{\partial x_j} = f_i - \frac{1}{\rho}\frac{\partial p}{\partial x_i} + v\frac{\partial^2 u_i}{\partial x_j \partial x_j} + \frac{1}{\rho}\frac{\tau_{ij}}{\partial x_j} \qquad\qquad [2]$$

Where $u_i(i=1,2,3)$ is average flow velocity, x_i is cartesian coordinate, ρ is water density, v is kinematic viscosity coefficient, p is pressure, f_i is volume force, τ_{ij} is

Reynolds stress. Reynolds stress is expressed as a linear equation of the standard $k - \varepsilon$ model.

2.2 Gravel transport model

The motion of the particle simulating the gravel was calculated by the equation of motion of Newton of the equation [1].

$$M \frac{du_p}{dt} = F_{Ds} + F_{Dus} + F_M + F_G + F_{ran} \qquad [3]$$

Where u_p is velocity of particle, M is mass of particle. As external forces acting on the particles to express drag F_D (stationary drag force F_{Ds} + unsteady drag force F_{Dus}), lifting force F_M, gravity, buoyancy F_G and external force F_{ran} to express irregular motion due to collision and rolling were considered. The handling of gravel was simplified, the particles were assumed to be perfectly spherical, and the volume, area, and mass were calculated by diameter and density of particles as analysis conditions.

2.2.1 Drag

The drag acting on the gravel always changes according to the flow field around the gravel and the fluid drag varies when the relative velocity between the gravel and the flow field is constant and varies. The fluid drag is divided into the stationary drag force F_{Ds} affected by the instantaneous relative velocity of the gravel and the flow field and the unsteady drag force F_{Dus} influenced by the time change of the relative velocity and are calculated by the following formula.

$$F_{Ds} = \frac{1}{2} C_D \rho_w u_r |u_r| A$$

$$F_{Dus} = C_M \rho_w \frac{\partial u_r}{\partial t} V \qquad [4]$$

$$u_r = u_w - u_p$$

Where ρ_w is the density of water, C_D is the drag coefficient, u_r is the relative flow velocity in each direction, u_w is the flow velocity of water at the particle center position, A is the projected area in each direction of the gravel, C_M is the inertial force coefficient (= 1.0), V is the volume of gravel. The drag coefficient was determined as a function of particle Reynolds number using the equation of Morsi and Alexander (1972) which is the resistance equation of a single sphere.

2.2.2 Lifting force (Magnus effect)

The gravel collides with the wall surface of the tunnel and causes rotational motion. Therefore, until the rotation speed of the gravel and the fluid become equal by the fluid viscosity, a relative angular velocity occurs between the gravel and the fluid. The following Magnus force was calculated as the lift acting on the gravel depending on the relative angular velocity.

$$F_{Mag} = \frac{1}{2} C_{Mag} A \rho_w |u_r| \frac{u_r \times \omega_r}{|\omega_r|}$$

$$\omega_r = \omega_p - \frac{1}{2} \cdot (\nabla \times u_w)$$

[5]

Where ω_r is the relative angular velocity of the particle and fluid, and C_{Mag} is the coefficient of rotational lift. C_{Mag} is calculated from the empirical formula and theoretical equation by Maccoll (1928), Davies (1970), Rubinow *et al.* (1961) and Osterle *et al.* (1998) using the function of the peripheral speed ratio of the particle surface rotation speed and relative velocity as follows.

$$C_{Mag} = 2\Gamma_p \qquad\qquad\qquad\qquad Re_p \leq 1$$
$$C_{Mag} = 0.45 + (2\Gamma_p - 0.45) \cdot \exp(-1.075\Gamma_p^{0.4} Re_p^{0.7}) \quad 10 \leq Re_p \leq 140 \quad and \quad 1 \leq \Gamma_p \leq 6 \text{ [6]}$$
$$C_{Mag} = \min[0.5, 0.5\Gamma_p] \qquad\qquad\qquad otherwise$$

2.2.3 Gravity and buoyancy

Gravity and buoyancy are calculated by the following equation using gravitational acceleration.

$$F_G = (\rho_d - \rho_w)gV$$

[7]

Where ρ_d is the density of soil (= 2.65 g/cm^3), and g is the gravitational acceleration.

2.2.4 External force to express irregular motion due to collision and rolling

When the gravel flows down through the tunnel, it collides with the bottom wall and the side walls and repeats irregular rolling. In this study, considering that very long calculation time is required for collision determination and calculation as the number of particles calculated increases, a random walk to simulate the influence of irregular motion due to collision was used. The external force F_{ran} for expressing the irregular motion of the gravel is calculated by the following formula.

$$F_{ran} = \sqrt{2D_{ran}}(2p_r - 1)$$

[8]

Where D_{ran} is a diffusion coefficient due to collision (= 0.03), and p_r is a random number obtained by random variable generation having an average of 0.5.

The above shows the model configuration in Table 1.

Table 1:   Model configuration

Flow model	3-dimensional non-hydrostatic analysis model
Free water surface	VOF (Volume of Fluid) method
Turbulence model	Standard $k - \varepsilon$ model
Gravel transport model	Consider the following forces as external forces acting on the gravel · Drag (steady drag + unsteady drag) · Lifting force · Buoyancy and gravity · Irregular external force caused by collision and rolling

2.3   Analysis condition

The calculated area was 2,350 m from the inlet to the outlet of the sediment bypass tunnel. The bed slope was 1/35 and the tunnel width was 3.8 m. For the calculated mesh size in the longitudinal direction of the tunnel, the interval of about 1200 m from the inlet of the sediment bypass tunnel to the front of the curved section was set at 10 m. The calculated mesh size from the curved section to the exit of the tunnel was set to 0.1 m in the transverse direction and 2m in the longitudinal direction, and the mesh interval was set to continuously change. The calculated mesh size in the vertical direction was 0.2 m in order to reproduce the flow in the tunnel at the time of free flow. Figure 2 shows the calculation mesh, and Figurer 3 shows the distribution of the elevation.

Two discharges of 50 m³/s as the normal discharge and 140 m³/s as the maximum discharge were set from the inlet of the sediment bypass tunnel. Free outflow conditions were set for the boundary condition of the downstream end of the tunnel.

As the particle size of the gravel, particle diameter of 1 cm as the minimum particle diameter, 7 cm as the average particle diameter and 20 cm as the maximum particle diameter was set from the results of the riverbed material investigation at Asahi Dam. Gravel particles were placed in the region of 2 m × tunnel width near 200 m upstream of the curved part of the tunnel. Figure 4 shows the placement of gravel particles.

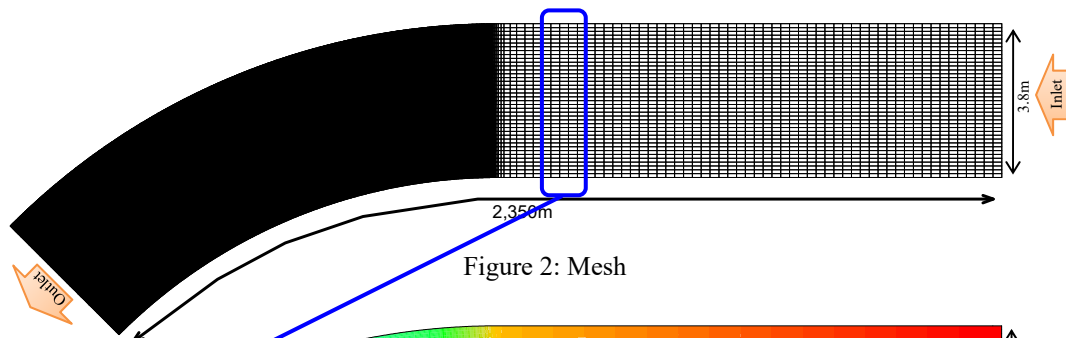These calculation conditions are summarized in Table 2.
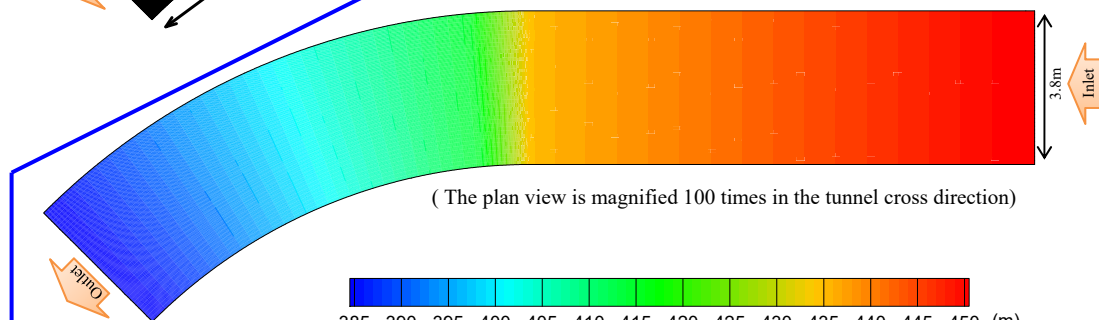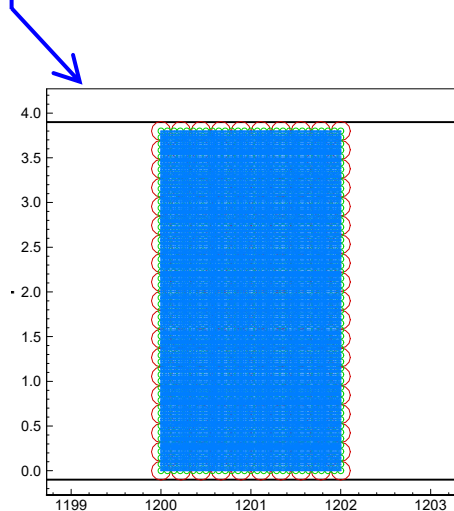
Figure 2: Mesh

(The plan view is magnified 100 times in the tunnel cross direction)

385 390 395 400 405 410 415 420 425 430 435 440 445 450 (m)

Figure 3: Elevation

Figure 4: Placement of gravel particles

Item	Condition
Calculation area	Sediment bypass tunnel 2,350m
Bed slope	1/35
Tunnel width	3.8m
Total mesh number	4,328,513
Mesh size	Δx : 2～10m Δy : 0.1m Δz : 0.2m
Discharge	normal discharge : 50m^3/s Maximum discharge : 140m^3/s
Particle size of gravel	1cm, 7cm, 20cm
Downstream end condition	Free outflow

Table 2: List of calculation conditions

3 Analysis result

3.1 Flow

Figure 5 shows the planar distribution of the flow velocities of the surface and the bottom in the bypass tunnel at discharge of 50 m^3/s and 140 m^3/s. Figure 6 shows the plane distribution of the flow velocity in the typical transverse plane (a: straight section, b: boundary from straight section to curved section, c: curved section) in the bypass tunnel at discharge of 50 m^3/s and 140 m^3/s. From the flow velocity distribution, the flow velocity distribution in the straight section is almost uniform in the transverse

direction. On the other hand, in the curved section, the flow velocity on the right bank, which is outside, increases and the flow velocity on the left bank inside the curve decreases. In the case of 140 m³/s, a flow toward the left bank occurs in the straight section to compensate for the flux of the inner flow caused by the flow from the inside toward the outside in the downstream curved section.
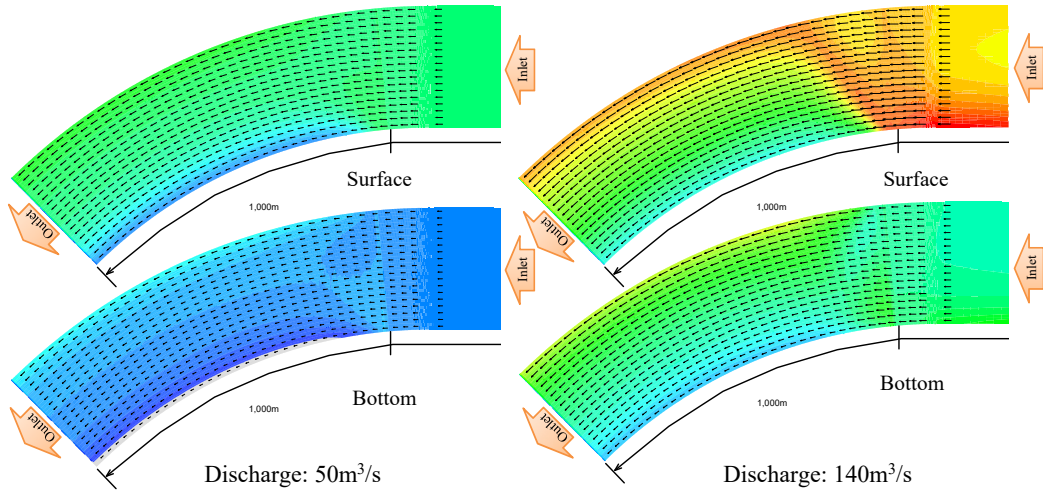

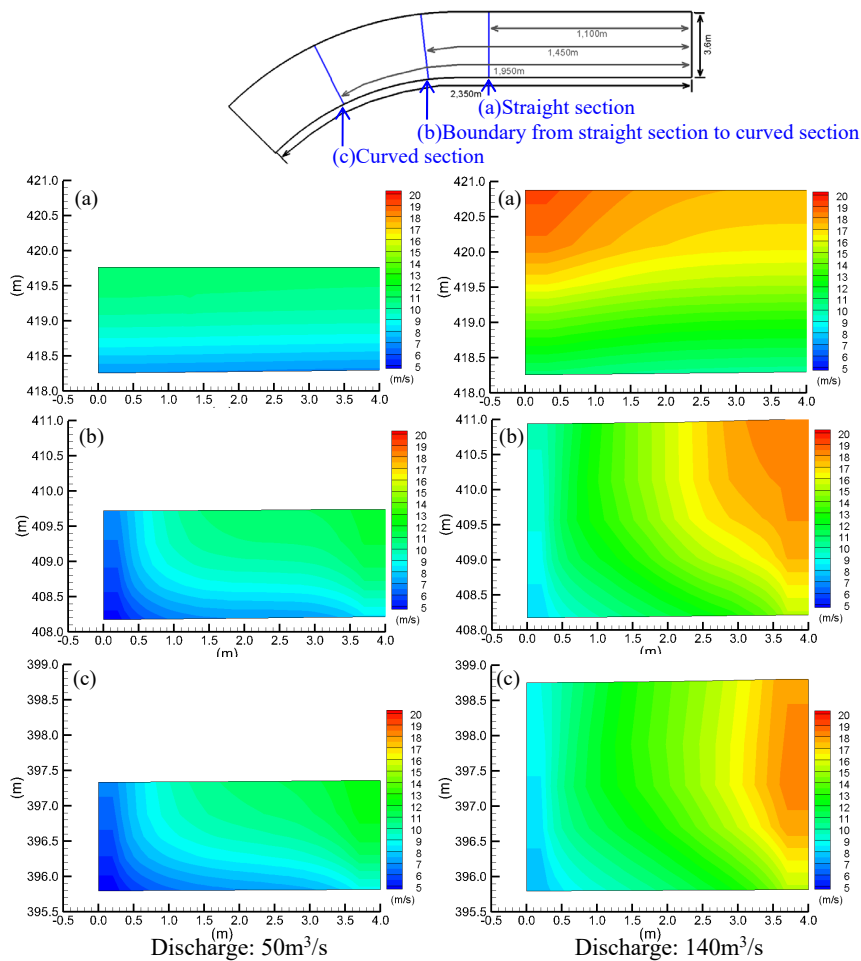Figure 5: Planar distribution of flow velocity

Figure 6: Transverse distribution of flow velocity

3.2   Movement of gravel particles

Figure 7 shows the migration results of each gravel particle at discharge of 50 m^3/s and 140 m^3/s. From the results, gravel with small grain size moves on the outside and moves outside the curved part of the tunnel with high flow velocity, and on the contrary the distribution range of gravel with large grain size expands due to the drag and the inside of the curved part the tunnel. The deviation of the movement path due to the difference in the particle diameter is more prominent in the case of the normal discharge of 50 m^3/s than the maximum discharge of 140 m^3/s.

Figure 8 shows the actual (accumulated value) of the abrasion depth of the concrete in the sediment bypass tunnel. From the figure, in the section from the inlet of the tunnel to the front of the curve, the wear depth is larger on the right bank side. On the other hand, in the curved section up to the tunnel exit, the abrasion depth on the left bank side is larger and the abrasion is larger than the straight section. Although the actual flow cannot be confirmed, abrasion in the straight section may be an influence of deviation of the inflow to the right bank.

Figure 9 shows the passing ratio of gravel particles in a typical cross section (a: straight section, b: boundary from straight section to curved section, c: curved section). The proportion of passing particles is calculated by dividing the number of passing particles at each transverse position by the total number of particles passing through the transverse section. As shown in Figure 9a, in the straight section, due to the influence of the flow deflected to the left bank before coming into the curved section, the distribution in the cross direction is slightly higher on the left bank side. As shown in Figure 9b, particles with a particle size of 1 cm pass much outside the curved section, whereas particles with a particle size of 20 cm pass through the inside of the curved section. In the curved section, particles with large volume move inside the curved section where the difference in flow speed is large due to the influence of inertial force and lift force. As shown in Figure 9c, small particles are biased to the outside of the curved section, and large particles are biased toward the inside of the curved section.

Figure 10 shows the Time series of the passing ratio of outflowing particles at the sediment bypass tunnel exit. The result is compared at the ratio of the number of particles at each time divided by the total number of particles flowed out. In the case of 50 m^3/s, the outflow of particles with a particle size of 1 cm is the fastest, and there is a large difference in the outflow time of particles of 20 cm. This is because particles of 1 cm pass through a region with a high flow velocity which is outside the curvature of the tunnel while particles of 20 cm pass through a region with a low flow velocity inside the curvature. In the case of 140 m^3/s, the larger the particle diameter, the faster the outflow time. In either case the outflow of particles continues with periodic oscillations. This is due to roll-wave occurring in the tunnel.
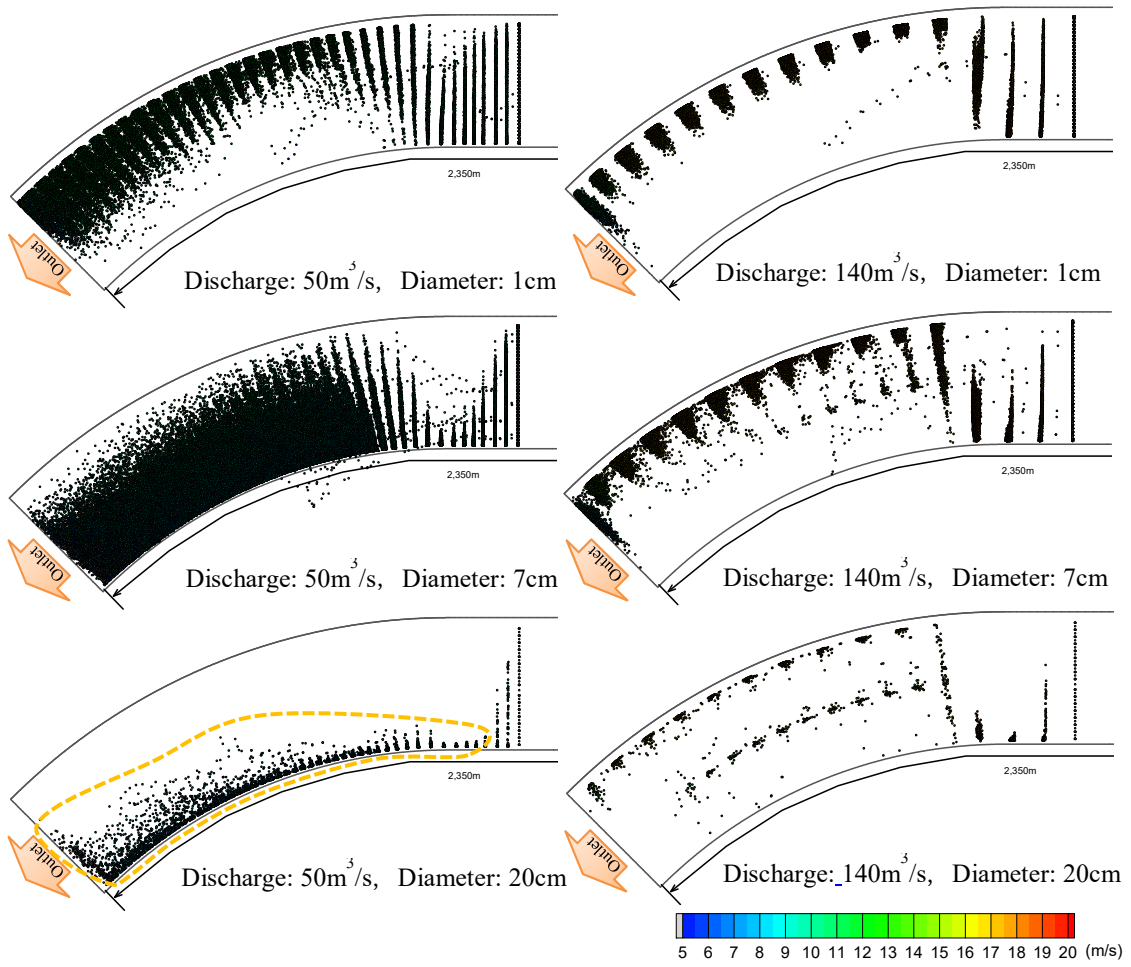
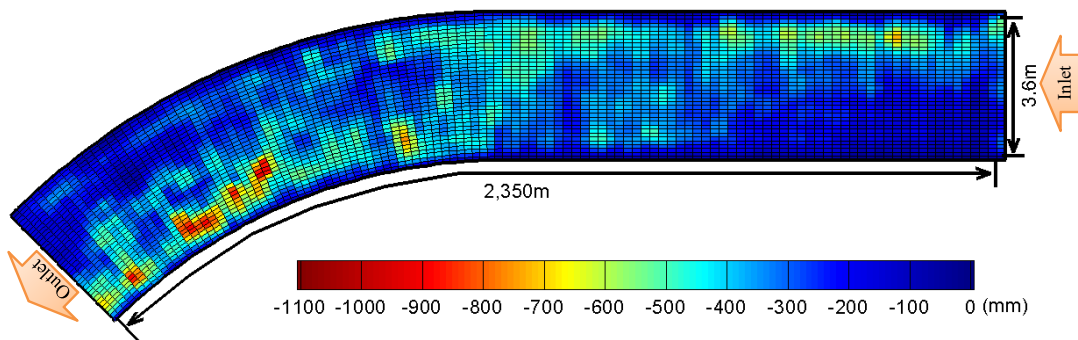Figure 7: Particle trajectory (about 5 second interval)

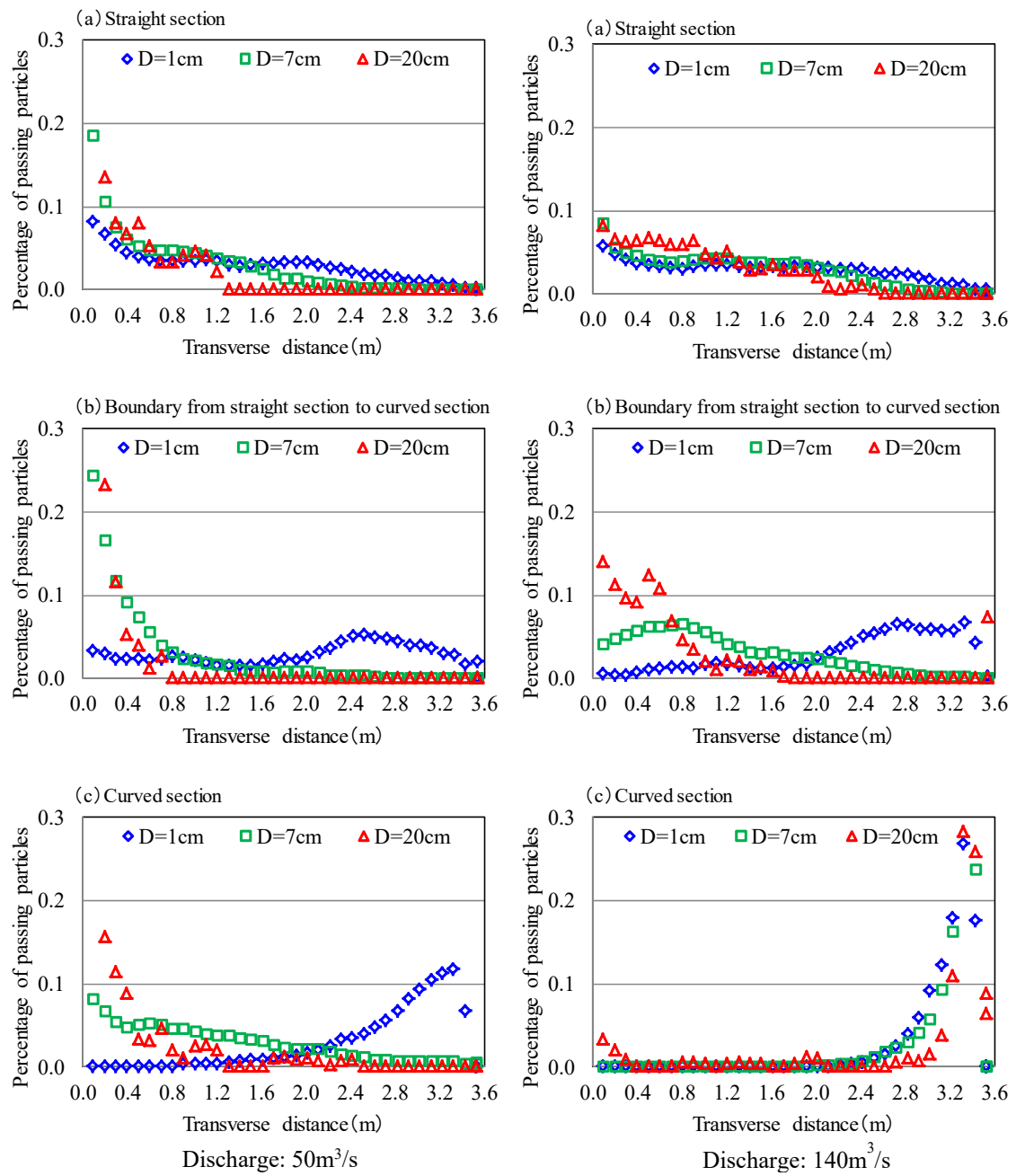Figure 8: Survey record of concrete abrasion depth (cumulative value)

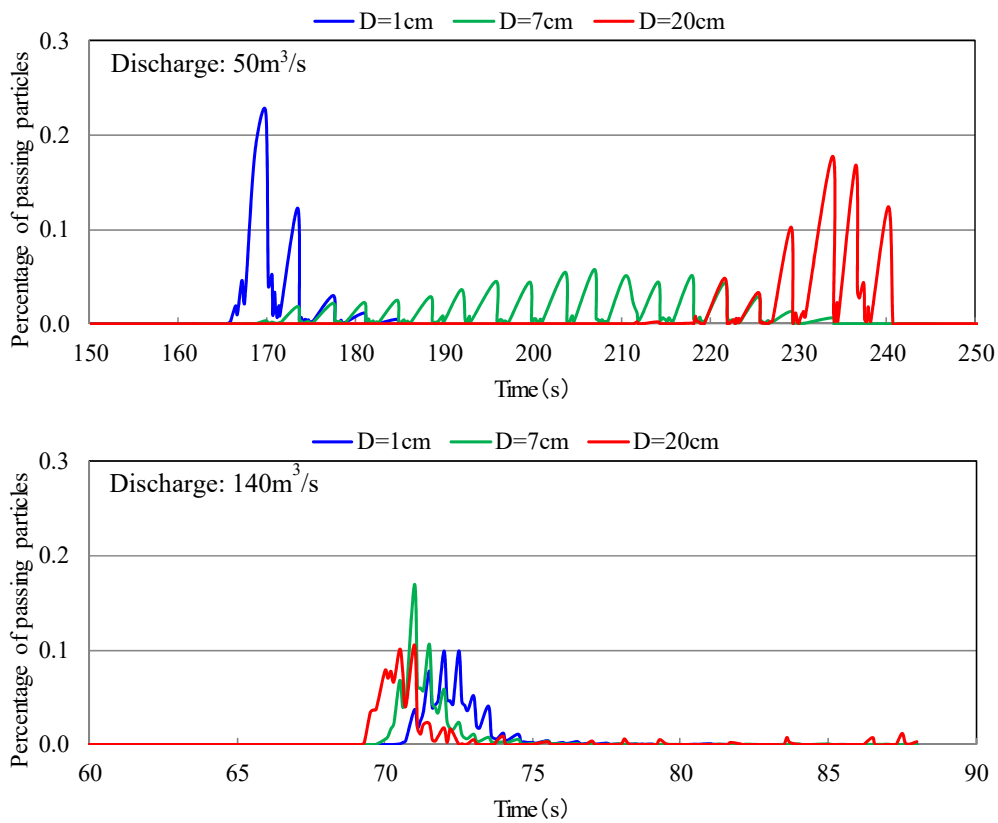Figure 9: Passing ratio of gravel particles in a typical cross section

Figure 10: Time series of the passing ratio of outflowing particles

4 Conclusion and future tasks

4.1 Conclusion

The large gravel mainly affects abrasion with a large impact force, so the abrasion region is similar to the movement route of a relatively large grain size. As a result of comparing the actual result (cumulative value) of the abrasion depth of concrete in the sediment bypass tunnel shown in Figure 3 with this analysis result, It was revealed that the migration path of the gravel with a particle size of 20 cm at a discharge of 50 m^3/s was substantially coincident with the area inside the curved section where abrasion was remarkable due to actual results. From the above, it was shown that this analysis method is effective for predicting the abrasion area in the tunnel.

4.2 Future tasks

As the next step, using the formula for estimating the amount of abrasion of the invert to the straight water channel proposed by Auel *et al*. (2014) by assuming the collision angle and collision speed. It is possible to estimate the amount of abrasion distribution in the tunnel.

Acknowledgement

References

Yoneyama, N., Inoue, M. (2001). Prediction method for water temperture and turbidity in pumped strage reservoir using 3D numerical simulation code, Proceedings of JSCE 684, 127-140. (in Japanese)

Kubota, Y., Yoneyama, N., Sumi, T. (2015). Diversion propaties of sediment bypass facilities using three-dimensional sediment transport model, *Journal of Japan Society of Civil Engineers, Ser.B1 (Hydraulic Engineering)*, 71(4), I_781-I_786. (in Japanese)

Morsi, S.A., Alexander, A.J. (1972). An investigation of particle trajectories in two-phase flow systems, *J. fluid Mech.*, 55, 2, pp.193-208.

Maccoll, J. (1928). Aerodynamics of a spinning sphere, *J. Roy. Aero. Soc.,* 32, pp.777-798.

Davis, J.W. (1970). The aerodynamics of golf balls, *J. Appl. Phys.*, 20, pp.821-828.

Rubinow, S.I., Keller, J.B. (1961). The transverse force on spinning sphere moving in a viscous fluid, J. *Fluid Mech.*, 11, pp.447-459.

Oesterle, B., Dinh, T.B (1998). Experiments on the lift of a spinning sphere in a range of intermediate Reynolds numbers, *Experiments in Fluids*, 25, pp.16-22.

Auel, C., Boes, R.M., Sumi, T. (2014). Abrasion damage estimation of sediment bypass tunnels: validation and comparison of two prediction models, *Annuals of Disaster Prevention Research Institute, Kyoto University*, 58, 540-549.

Authors

Yoji Kubota (corresponding Author)
Hydro-soft Technology Institute Co., Ltd., Japan
Email: kubotayj@hydro-soft.co.jp

Nozomu Yoneyama
Tetsuya Sumi
Disaster Prevention Research Institute, Kyoto University, Japan